New Insights into the Solution Behavior of Cobalamins. Studies of the Base-Off Form of Coenzyme B_{12} Using Modern Two-Dimensional NMR Methods

Ad Bax,[†] Luigi G. Marzilli,[‡] and Michael F. Summers*[§]

Contribution from the Laboratory of Chemical Physics, National Institute of Arthritis, Diabetes and Digestive and Kidney Diseases, National Institutes of Health, Bethesda, Maryland 20892, the Department of Chemistry, Emory University, Atlanta, Georgia 30322, and the Biophysics Laboratory, Center for Drugs and Biologics, Food and Drug Administration, Bethesda, Maryland 20892. *Received June 19, 1986*

Abstract: Recently developed two-dimensional (2D) NMR methods are used to assign completely the ^1H and ^{13}C NMR spectra of the base-off form of coenzyme B_{12} (5′-deoxyadenosylcobalamin, M_r = 1580). The NMR data, including coupling constants, chemical shifts, 2D proton–carbon multiple-bond peak intensities, and 2D NOE peak intensities, are compared with those of the base-on form of coenzyme B_{12} and with the structure recently determined by neutron diffraction. The NOE signal intensities between protons of the corrin and adenosyl indicate a dynamic equilibrium between at least two states: in one state, the orientation of the adenosyl with respect to the corrin is similar to that observed in the crystal structure, and in the other state, the adenosyl is rotated ca. 50° counterclockwise (when viewed from the adenosyl) about the Co–C bond. Furthermore, we find no evidence for a change in corrin ring pucker on dissociation of the 5,6-dimethylbenzimidazole (DMBz). For the base-off species, the DMBz is repositioned "upside down" with the B7, B11, and R1 protons in the vicinity of the C20 methyl group. Previously unexplainable shift trends in the base-on to base-off conversion are more readily rationalized by use of the new data since, in earlier studies, errors were made both in assigning some of the signals of the base-on form and in following the shift of some of the signals with changes in pH. The protonated nucleotide loop in the base-off form has ^{13}C chemical shifts similar to those of the protonated nucleotide, ribazole-3′-phosphate. The changes in chemical shifts and coupling constants in the ribose moiety of the loop suggest a change in conformation on formation of the base-off form. The primary effects on the side-chain signals of the base-on to base-off conversion are for the signals of the *e*-propionamide side chain. Relatively little effect is found for the A ring side-chain signals, and intermediate effects are found for the B and D ring side chains. Thus, from the base-off ^{13}C data, there appears to be no reason for concluding that the "eastern" half of the corrin (rings B and C) is more flexible.

5′-Deoxyadenosylcobalamin (coenzyme B_{12}, M_r = 1580) is a cofactor in over a dozen enzymatic reactions, two of which are known to be important in humans.[1] It is now generally believed that an essential early step in the catalytic cycle is the homolysis of the bond between Co and the A15 carbon of deoxyadenosyl (Chart I).[2-4] The coenzyme is relatively stable to thermolytic homolysis, and it is clear that Co–C bond cleavage is induced by steric or electronic effects or a combination of both. In a recent review, several "mechanisms" were discussed in terms of their possible importance in the triggering of Co–C bond homolysis.[3] Four of these included, in some regard, steric interactions between the 5′-deoxyadenosyl moiety and the corrin ring. In two putative mechanisms, steric interactions were affected by a repositioning of the 5,6-dimethylbenzimidazole (DMBz) ligand. In this regard, UV data have been interpreted to indicate that, during catalysis, the cobalt-to-DMBz bond is broken.[5] In addition, analysis of ^{13}C NMR chemical shifts has led to speculation that the DMBz experiences "steric compression" with side chains of the corrin ring[6,7] and that the "eastern" half of the molecule (rings B and C) is more flexible than the "western" half.[8]

The strength of the Co–C bond in organocobalt compounds is directly related to the electron-donor ability of the trans axial ligand.[2] Bulky alkyl groups generally lead to steric interactions with the equatorial ligand, which lengthen and weaken the Co–C bond.[2,3] However, new X-ray structural data on methylcobalamin reveal a corrin conformation similar to that of coenzyme B_{12} and suggest that there is relatively little steric strain between the 5′-deoxyadenosyl group and the corrin ring.[9] In a more recent hypothesis, the Co–N(DMBz) bond is lengthened in the holoenzyme. Then the role of the DMBz is to act as a poor electron donor that weakens the trans Co–C bond by insufficiently stabilizing the electron-deficient Co(III) oxidation state. Subsequent to homolysis, the DMBz stabilizes the Co(II) intermediate through its (possibly shorter) bond to Co.[10] In this case, direct steric interactions between the corrin and the DMBz are unimportant in weakening the Co–C bond. In a molecule as complex as coenzyme B_{12}, however, any number of the various hypothesized triggering mechanisms could, to some degree, act in concert to facilitate Co–C bond homolysis.

At least two approaches can be employed to study the role of the DMBz: X-ray crystallography and NMR spectroscopy. Unfortunately, X-ray quality crystals of alkylcobalamins have been difficult to obtain, and no good crystals have been obtained for a cobalamin in the base-off form or in a holoenzyme. Furthermore, the size of cobalamins is such that highly accurate distances and angles cannot be obtained by current diffraction methods, and this problem is exacerbated in enzymes and proteins. Therefore, we are exploring the application of modern two-dimensional (2D) NMR spectroscopic methods in order to examine electronic and structural properties of alkylcobalamins. One of the main advantages 2D NMR offers over 1D NMR is the

* To whom correspondence should be addressed.
† Laboratory of Chemical Physics.
‡ Emory University.
§ Biophysics Laboratory.

(1) *B_{12}*; Dolphin, D., Ed.; Wiley: New York, 1982; 2 vols.
(2) Halpern, J. *Science (Washington, D.C.)* **1985**, *227*, 69.
(3) Bresciani-Pahor, N.; Forcolin, M.; Marzilli, L. G.; Randaccio, L.; Summers, M. F.; Toscano, P. J. *Coord. Chem. Rev.* **1985**, *63*, 1.
(4) Finke, R. G.; Schiraldi, D. A.; Mayer, B. J. *Coord. Chem. Rev.* **1984**, *54*, 1.
(5) Pratt, J. M. *Inorg. Chim. Acta* **1983**, *79*, 27.
(6) Hensens, O. D.; Hill, H. A. O.; McClelland, C. E.; Williams, R. J. P. In *B_{12}*; Dolphin, D., Ed.; Wiley: New York, 1982; Vol. 1, p 463 and references therein.
(7) Hogenkamp, H. P. C.; Thachuk, R. D.; Grant, M. E.; Fuendes, R.; Matwiyoff, N. A. *Biochemistry* **1975**, *14*, 3707.
(8) Bratt, G. T.; Hogenkamp, H. P. C. *Biochemistry* **1984**, *23*, 5653.
(9) Rossi, M.; Glusker, J. P.; Randaccio, L.; Summers, M. F.; Toscano, P. J.; Marzilli, L. G. *J. Am. Chem. Soc.* **1985**, *107*, 1729.
(10) Marzilli, L. G.; Summers, M. F.; Bresciani-Pahor, N.; Zangrando, E.; Charland, J.-P.; Randaccio, L. *J. Am. Chem. Soc.* **1985**, *107*, 6880.

0002-7863/87/1509-0566$01.50/0

Chart I

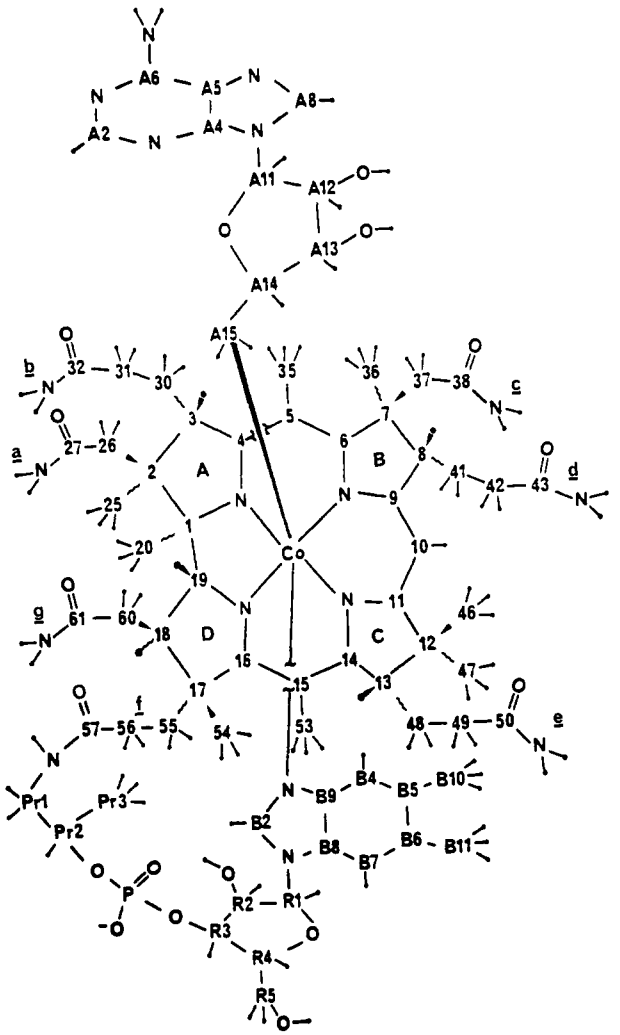

disentanglement of overlapping resonances by spreading the spectrum in two independent frequency dimensions. In a previous study,[11] the application of Homonuclear Hartmann–Hahn (HOHAHA), spin-locked 2D NOE, ^1H–^{31}P spin-echo difference, and COSY NMR spectroscopies led to the complete ^1H NMR assignment of 5′-deoxyadenosylcobalamin at pH 7. The subsequent application of heteronuclear multiple quantum coherence (HMQC) and heteronuclear multiple bond multiple quantum coherence (HMBC) spectroscopies led to complete assignment of the ^{13}C NMR signals.[11,12] In the present study, these methods are extended, but with a slightly different and more expedient approach, to the study of the base-off form of coenzyme B_{12}.

NMR Methods and Spectra

The NMR experiments and pulse sequences employed here are the same as those used in a previous study of the base-on form of coenzyme B_{12}.[11] Homonuclear Hartmann–Hahn spectroscopy (HOHAHA)[13-17] is used to group proton signals into *J*-coupled networks. For example, Pr1H′, Pr1H″, Pr2H, and Pr3H_3 (for nonequivalent geminal protons, H′ and H″ refer to protons with the downfield and upfield signals, respectively) belong to a *J*-

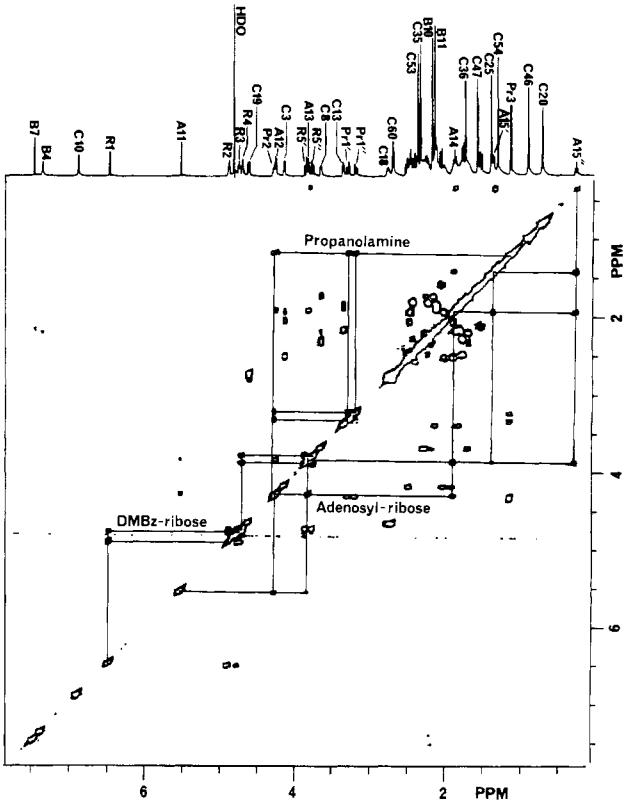

Figure 1. Part of the phase-sensitive 2D HOHAHA spectrum of the base-off form of coenzyme B_{12}, obtained with a 57-ms MLEV-17 spin-lock mixing period. The *J*-connectivities for the two ribose ring protons and the propanolamine protons are indicated by drawn lines. Other connectivity patterns are indicated in the supplementary material.

network as shown in the HOHAHA spectrum in Figure 1. The HOHAHA experiment is similar to the conventional COSY experiment (supplementary material) in that it provides connectivities between *J*-coupled spins; however, the COSY data reveal only direct coupling whereas the HOHAHA data contain direct and relayed *J*-coupling information. During the mixing period of the HOHAHA experiment, magnetization is transferred from one proton (A) to another (M) at a rate proportional to the coupling constant (J_{AM}). If proton M is coupled to a third proton, X, the magnetization of A can be relayed to X via the M nucleus. For intermediate to long mixing periods, magnetization from one proton will be distributed over most or all of the other protons in the same coupling network. This experiment is especially important where signals from two or more *J*-networks overlap, making analysis on the basis of the conventional COSY experiment alone virtually impossible.

Spin-locked 2D NOE spectroscopy[18] is employed to provide through-space connectivity between protons of different *J*-networks and also for structural analysis. The 2D NOE spectrum is given in Figure 2. There are a number of advantages in using the spin-locked experiment relative to the conventional 2D NOE experiment. First, at our field strength (11.75 T) the regular 2D NOE experiment gives weak cross peaks relative to the spin-locked experiment due to the fact that the molecular tumbling time, τ_c, for coenzyme B_{12} is close to the reciprocal of the angular Larmor frequency, ω_L. A second advantage of the spin-locked experiment is that relayed NOE signals (from A to X via M) are inverted relative to direct NOE singals. The differentiation of direct and indirect NOEs is very important if structural interpretations are to be made.

For correlating protons and carbons, two types of ^1H-detected heteronuclear multiple quantum NMR experiments were per-

(11) Summers, M. F.; Marzilli, L. G.; Bax, A. *J. Am. Chem. Soc.* **1986**, *108*, 4285.
(12) Bax, A.; Summers, M. F. *J. Am. Chem. Soc.* **1986**, *108*, 2093.
(13) Braunschweiler, L.; Ernst, R. R. *J. Magn. Reson.* **1983**, *53*, 521.
(14) Davis, D. G.; Bax, A. *J. Am. Chem. Soc.* **1985**, *107*, 2820.
(15) Davis, D. G.; Bax, A. *J. Am. Chem. Soc.* **1985**, *107*, 7197.
(16) Bax, A.; Davis, D. G. *J. Magn. Reson.* **1985**, *65*, 355.
(17) Bax, A.; Davis, D. G. In *Advanced Magnetic Resonance Techniques in Systems of High Molecular Complexity*; Nicolai, N., Valensin, G., Eds.; Birkhauser: Boston, 1986; p 21.

(18) Bothner-By, A.; Stephens, R. L.; Lee, J. T.; Warren, C. D.; Jeanloz, R. W. *J. Am. Chem. Soc.* **1984**, *106*, 811. Davis, D.; Bax, A. *J. Magn. Reson.* **1985**, *63*, 207.

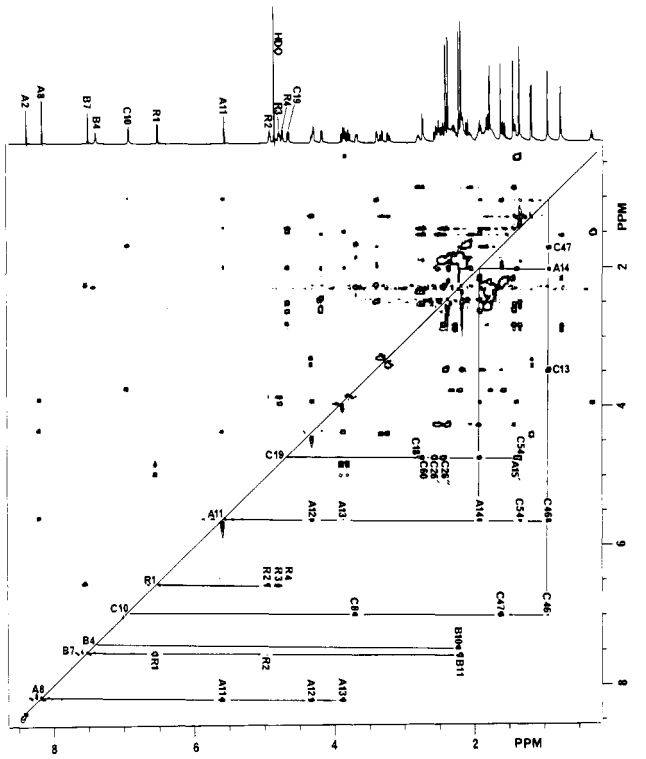

Figure 2. Part of the absorption mode 2D spin-locked NOE spectrum of the base-off form of coenzyme B_{12}, obtained with a 200-ms spin-lock period. Connectivity patterns for the low-field proton signals and some of the cross peak signals of structural relevance are indicated (see text for details).

formed. One-bond (^1J) connectivities were made by using the "BIRD-modified" HMQC (heteronuclear multiple quantum correlation) pulse sequence, and multiple-bond (^2J and ^3J) connectivities were established by using the HMBC (heteronuclear multiple bond correlation) sequence, both of which have been described in detail previously.[12,19] Figure 3 shows the upfield ^{13}C region of the HMQC spectrum, and Figure 4 shows part of the upfield ^{13}C region of the HMBC spectrum; the remaining regions of these spectra are given in the supplementary material. The HMBC experiment correlates signals of protons and ^{13}C nuclei that have a significant long-range scalar coupling interaction (> ca. 3 Hz). Under the conditions employed, it was impossible to differentiate between two- and three-bond couplings.[20] Due to limitations in the ^{13}C radio frequency power, the HMQC and HMBC experimental data were obtained in two sets: one with the ^{13}C radio frequency (rf) carrier at 60 ppm and the other with the carrier at 145 ppm. As will be shown below, the HMQC and HMBC data can be used in concert to make proton and carbon assignments simultaneously.

Two-dimensional ^1H–^1H J-resolved (2D-J) spectroscopy[21] was employed to determine accurate ^1H–^1H and ^1H–^{31}P coupling constants for signals of base-on and base-off B_{12}. Part of the 2D-J spectrum of base-off B_{12} is given in Figure 6, and the spectrum for base-on B_{12} is given in the supplementary material.

Signal Assignment Procedure

In our study of base-on B_{12}, the ^1H spectrum was assigned first followed by assignment of the ^{13}C spectrum.[11] Extensive ^1H–^1H coupling and signal overlap made the initial ^1H assignment tedious to perform and time consuming. A simpler approach, we have found, is to use the HMQC and HMBC data to simultaneously assign protons and carbons in a stepwise manner, beginning at a known starting point on the corrin ring. This approach is demonstrated briefly below.

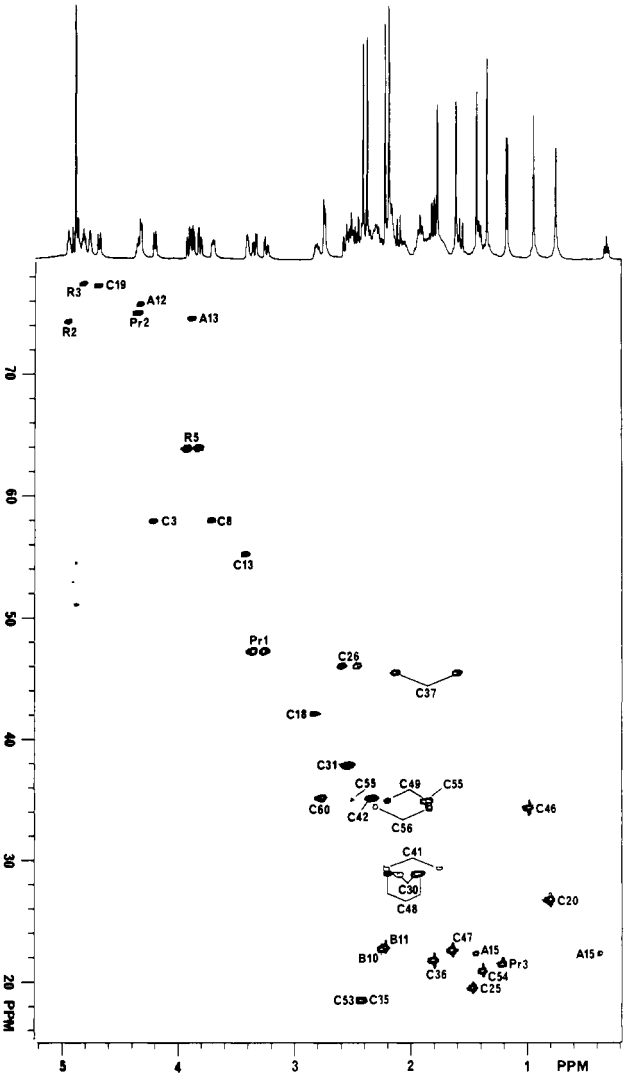

Figure 3. Part of the high-field (^{13}C) absorption mode ^1H-detected ^1H–^{13}C correlation spectrum of base-off B_{12}. The corresponding region of a conventional 1D proton spectrum is shown at the top of the figure for clarification. The labeled peaks correlate signals between protons and directly attached carbons. The downfield (^{13}C) region is given in the supplementary material.

Many intense multiple-bond ^1H–^{13}C cross peaks can be seen in the upfield carbon region of the HMBC spectrum, Figure 4. The easiest starting point for signal assignments on the corrin ring is at C12. This is the only carbon in the molecule which has two methyl groups (C46 and C47) attached, and as such the protons of one methyl group should give an HMBC correlation peak with the carbon signal of the other methyl group. Of the nine methyl signals observed, only the ^1H signals at 1.00 and 1.67 ppm have ^3J correlation peaks with each others respective ^{13}C signal (22.3 and 33.7 ppm, respectively; Figure 4), assigning these protons (not specifically) to C46 and C47. Since the 1.00 ppm signal displays an NOE cross peak with protons of the 5′-deoxyadenosyl moiety (vide infra), this signal is assigned to C46. The C46 and C47 methyl protons also have common correlation peaks with carbon signals at 49.5 and 55.4 ppm. By comparison with the HMQC data in Figure 3, the 49.5 and 55.4 ppm signals can easily be assigned C12 and C13, respectively, since the 49.5 ppm ^{13}C signal does not have an associated ^1H signal. In addition, the HMQC correlation peak at 55.4 ppm (^{13}C, Figure 3) directly gives the C13H chemical shift as 3.43 ppm.

As for the base-on form of coenzyme B_{12}, C13H gave weak HMBC correlation peaks. However, at the lower contour levels displayed in the left half of Figure 4, two correlation peaks are

(19) Bax, A.; Subramanian, S. *J. Magn. Reson.* **1986**, *67*, 565.
(20) At higher digital resolution ^2J and ^3J HMBC signals can be distinguished.
(21) Aue, W. P.; Karhan, J.; Ernst, R. R. *J. Chem. Phys.* **1976**, *65*, 4226. Hall, L. D.; Sukumar, S. *J. Magn. Reson.* **1980**, *38*, 555.

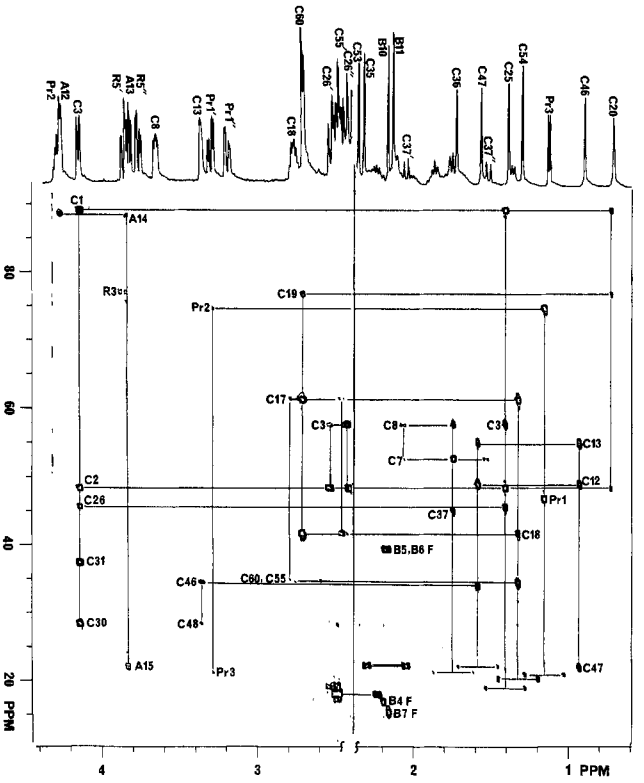

Figure 4. Part of the absolute value mode ^1H–^{13}C multiple-bond-shift correlation spectrum of base-off B_{12}. Corresponding regions of the 1D ^1H spectrum are shown at the top of the figure. Correlation peaks are due to multiple-bond connectivity between ^{13}C nuclei (signals labeled in the contour plot) and protons (labeled in the 1D spectrum). Lines have been added for clarification of the signal assignment procedure as described in the text. The lowest contour level for the part of the figure to the left side of the center line is 3 times lower than the region to the right of the center line. Signals folded in the ^{13}C dimension are labeled "F". Incompletely suppressed "satellite" peaks from intense methyl group signals (except C46 and C20) are also observed, which represent one-bond connectivity.

observed with C13H at 34.4 (C46) and 28.9 ppm (C48, assigned by using the HOHAHA data). In the downfield ^{13}C region of the HMBC spectrum (supplementary material), C13H, C48H′, and methyl protons at 2.46 ppm show correlation peaks to a common carbon signal at 166.7 ppm, assigning the carbon signal to C14 and the methyl protons to $C53H_3$.

The above procedure was followed until nearly all of the proton and carbon signals of the corrin ring were assigned. Thus, $C53H_3$ gives an HMBC correlation peak with C16; $C54H_3$ correlates with C16 and C18; C18H correlates with C60; $C60H_2$ correlates with C19; $C20H_3$ correlates with C19, C1, and C2; $C25H_3$ correlates with C1, C2, C3, and C26; C3H correlates with C1, C2, C26, and C4; $C35H_3$ correlates with C4, C5, and C6; and $C36H_3$ correlates with C6, C7, and C8. These and other HMBC correlations observed for the corrin and its substituents are shown in Figure 5. The C10H signal is broad at pH 2.1 and does not give rise to HMBC signals. In addition, C8H gives relatively weak HMBC correlation peaks and does not give a correlation peak with C10 (this was also the case for the base-on form). However, the C10H signal (6.97 ppm) could be identified on the basis of NOE cross peaks with C8H, $C46H_3$, and $C47H_3$ (see below). The C10 carbon assignment (100.4 ppm) then followed from the HMQC data. The unassigned proton and carbon signals of the corrin side chains were then assigned by first establishing the *J*-connectivity networks from the HOHAHA spectrum (Figure 1) as described previously and then assigning the protons and carbons by comparison to the HMQC spectrum. Where possible (i.e., where signal overlap was not severe), direct proton–proton connectivities were confirmed from the COSY spectrum (supplementary material). The carbonyl ^{13}C signals were assigned

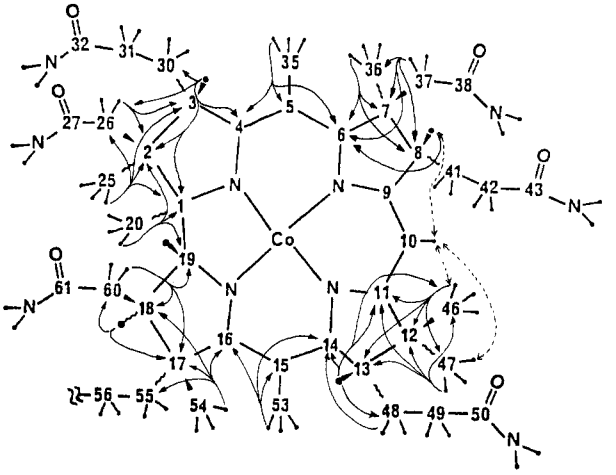

Figure 5. Drawing showing some of the HMBC connectivities (solid arrows) used to make ^1H and ^{13}C signal assignments for nuclei of the corrin macrocycle. The C10 proton signal did not give HMBC correlation peaks (see text), and assignment of this proton was made using 2D NOE connectivities (dashed arrows).

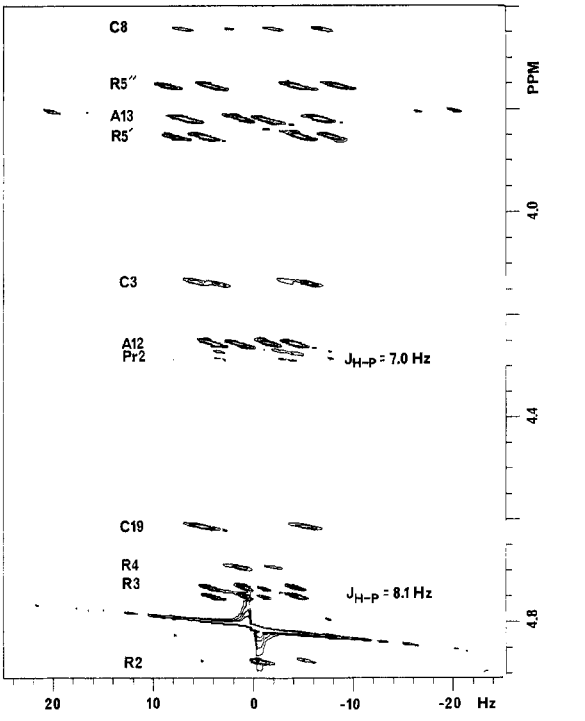

Figure 6. Part of the 2D *J*-resolved spectrum of base-off B12 which allowed assignment of ^1H–^1H and ^1H–^{31}P coupling constants.

from the downfield HMBC data (supplementary material). Proton and carbon signals of the axial ligands were similarly assigned by using the above procedure; here, we found it unnecessary to perform a ^1H–^{31}P spin-echo difference experiment as was done previously,[11] since the Pr1, Pr2, and Pr3 protons give a characteristic HOHAHA pattern and since Pr1H gives a ^3J correlation peak to C57 (Figure 5). Finally the 2D NOE data (Figure 6) were completely analyzed and found to be consistent with all of the ^1H assignments. The HMBC, HMQC, HOHAHA, and NOE connectivities are summarized in Table SI of the supplementary material. Chemical shifts and coupling constants are summarized in Tables I and II, respectively.

^{13}C Chemical Shifts

Since a substantial number of ^{13}C signals previously have been assigned incorrectly, we begin this discussion section by reevaluating the most extensive previous study on ^{13}C shift changes which

Table I. ^{1}H and ^{13}C NMR Chemical Shifts (ppm) and Signal Assignments for the Base-Off Form of 5'-Deoxyadenosylcobalamin[a]

	^{13}C NMR		^{1}H NMR
assignment	pH* 2.1	pH* 7.0	pH* 2.1
C35	18.4	18.3	2.43
C53	18.4	18.8	2.46
C25	19.4	19.9	1.48
C54	20.8	19.6	1.40
Pr3	21.5	21.7	1.23
C36	21.8	21.7	1.82
A15	22.3	27.3	1.46, 0.38
C47	22.6	23.9	1.67
B10	22.6	22.5	2.26
B11	22.7	22.3	2.23
C20	26.7	23.5	0.81
C48	28.9	30.3	2.21, 1.92
C30	29.0	29.2	2.11, 1.97
C41	29.4	28.7	2.21, 1.75
C46	34.4	34.2	1.00
C56	34.4	34.4	2.31, 1.85
C49	35.0	38.1	2.21, 1.86
C55	35.2	34.6	2.51, 1.85
C42	35.2	34.8	2.35
C60	35.2	34.8	2.78
C31	37.9	38.3	2.55
C18	42.2	42.5	2.85
C37	45.6	45.3	2.61, 2.14
C26	46.2	46.2	2.60, 2.46
C2	47.4	49.5	
Pr1	48.9	47.8	3.38, 3.27
C12	49.5	49.5	
C7	53.2	53.1	
C13	55.4	55.8	3.43
C3	58.1	58.5	4.23
C8	58.1	57.5	3.73
C17	61.8	60.8	
R5	64.1	63.4	3.94, 3.84
R2	74.5	72.0	4.97
A13	74.9	76.6	3.90
Pr2	75.2	76.0	4.36
A12	76.0	75.6	4.34
C19	77.6	76.8	4.70
R3	77.6	76.2	4.83
A14	88.9	88.6	1.98
R4	89.2	84.6	4.79
C1	89.8	88.5	
R1	90.2	89.4	6.56
A11	91.1	91.0	5.61
C10	100.4	97.7	6.97
C15	109.8	106.9	
C5	111.2	108.4	
B7	115.7	113.5	7.55
B4	117.2	121.4	7.44
A5	121.5	121.8	
B8	132.1	133.3	
B9	132.6	141.0	
B6	139.6	136.8	
B5	139.6	134.5	
B2	141.4	144.7	9.16
A8	145.5	143.8	8.21
A2	148.4	156.0	8.43
A4	151.0	151.8	
A6	153.5	158.7	
C6	166.2	166.6	
C14	166.7	167.2	
C9	175.1	173.1	
C38	177.4	177.9	
C57	178.3	178.2	
C11	179.0	177.6	
C61	179.1	179.0	
C27	179.1	179.3	
C4	179.4	178.7	
C16	179.4	178.7	
C43	180.9	180.3	
C50	181.0	181.1	
C32	181.1	181.1	

[a] Shifts relative to internal trimethylsilyl propionate; T = 20.0 °C.

accompany the base-on to base-off conversion.[8] In this section, we first will consider the ^{13}C signals as grouped together by C type as suggested by Bratt and Hogenkamp.[8] Next, we will consider the consequences of our reassignments on the interpretation of ^{13}C shifts as a function of the upper axial ligand.

Table II. Selected ^{1}H–^{1}H, ^{1}H–^{31}P, and ^{31}P–^{13}C Coupling Constants (Hz) for the Base-On and Base-Off Forms of Coenzyme B_{12}[a]

coupled spins	base-on	base-off
	^{1}H–^{1}H	
C19–C18	10.5	10.2
Pr1′–Pr1″	13.9	14.1
Pr1′–Pr2	<0.9	5.2
Pr1″–Pr2	14.4	3.9
Pr2–Pr3	6.3	6.3
R1–R2	3.0	5.2
R2–R3	4.3	5.1
R3–R4	8.9	3.3
R4–R5′	2.7	3.1
R4–R5″	3.9	4.3
R′–R5″	13.0	12.6
A11–A12	3.3	2.5
A12–A13	5.8	5.5
A13–A14	6.7	7.7
A14–A15′	<2.0	<2.0
A14–A15″	9.2	8.9
A15′–A15″	9.2	8.9
	^{1}H–^{31}P	
R2–P	<0.9	<0.9
R3–P	7.4	8.1
R4–P	<0.9	<0.9
Pr1–P	<0.9	<0.9
Pr2–P	7.1	7.0
Pr3–P	<0.9	<0.9
	^{13}C–^{31}P	
R2–P	<0.9	3.3
R3–P	3.7	4.4
R4–P	9.1	2.6
Pr1–P	<0.9	<0.9
Pr2–P	5.8	5.5
Pr3–P	4.4	3.3

[a] Coupling constants to ±0.1 Hz.

Base-On to Base-Off Conversion

Carbonyl and Imine Region. The 13 most downfield resonances (>160 ppm) were attributed to six nonprotonated pyrollidine carbons (4, 6, 9, 11, 14, and 16) and seven carbonyl carbons (27, 32, 38, 43, 50, 57, and 61). The previous assignments for the base-on form were correct except for C38 and C57, which were interchanged. On protonation, the carbonyl signals did not shift appreciably except for C43, in agreement with our data.

For the imine carbons, we agree that the on-to-off conversion shifts C14 upfield. However, we disagree with the interpretation of the titration results that the signals for C14 and C6 cross at pH 3.3 (see Figure 4 of ref 8). Thus, our results suggest that the shifts on protonation are small for both C14 and C6.

Nucleoside and Nucleotide Region. Our results and assignments for B2, B4, B8, B9, A2, A4, A5, and A6 agree with the previous work, and the base-on to base-off conversion leads to upfield shifts. The signals for A8, B5, B6, and B7 shift downfield.[22] These changes in chemical shift reflect not only the base-on to base-off conversion but also protonation of A1 and B3. ^{13}C signals for the ribose attached to DMBz undergo appreciable downfield shifts on protonation of DMBz. The Pr1 signal also shifts downfield, whereas Pr2 and Pr3 signals shift upfield. Previously, assignments for Pr2 and R2 were interchanged, and Pr1 was reported to shift upfield on protonation. Our results confirm the expected large upfield shift for A15 (bound to Co) on DMBz dissociation. As found previously,[8] A11, A12, and A14 signals shift slightly downfield and A13 shifts slightly upfield. Previously, A12 and A13 assignments were interchanged; however, little change appears to be occurring in the adenosyl sugar conformation as judged by ^{13}C shifts.

(22) B5 and B6 assignments were based on the assumption that the B4H-B6 and B7H-B5 couplings are larger than the B7H-B6 and B4H-B5 couplings.

Upfield Corrin Ring Region. Our assignments for the remaining 13 corrin ring carbons (1, 2, 3, 5, 7, 8, 10, 12, 13, 15, 17, 18, and 19) for the base-on form agree with the literature[8] values. The shifts on protonation are in excellent agreement except for C2, which appears to have been interchanged with Pr1. As found previously,[8] the major effect of the base-on to base-off conversion is on C5, C10, and C15.

Methylene Carbon Region. Previously, many signals in this region were incorrectly assigned, and indeed, it was stated that many of the assignments were tentative.[8] For the acetamide signals, C60 and C37 shift downfield (0.4 and 0.3 ppm, respectively) and C26 does not shift on protonation. In the previous work, C26 and C37 were interchanged. For the propionamide methylene carbons, we agree with earlier assignments for the base-on form; however, previously the assignments for C41 and C48 were incorrectly interchanged for the protonated form. Thus, we find an appreciable downfield shift of C41 and substantial upfield shifts for C48 and C49 on protonation. The substantial change in C41, which our results now reveal, is in agreement with Glusker's view,[23] based on X-ray crystallographic data, that C41, C48, C55, and C56 hold the DMBz in place. The significant upfield shift for C49 (3.1 ppm) indicates that this side chain may undergo reorientation on DMBz dissociation, perhaps due to loss of steric interactions with the DMBz and its attached ribose. The unusual upfield shift for one of the C49 geminal protons (see below) suggests that C49 may be repositioned underneath the corrin macrocycle. The relatively small changes in chemical shift for the C30 and C31 signals are attributable to the distance of this chain from the DMBz group. Our new assignments of C42, C55, and C56 signals indicate that the signals for the carbons attached to the corrin ring, C55 and C41, shift moderately downfield on DMBz dissociation whereas signals for carbons further out on the propionamide chains, C42 and C56, are less affected.

Methyl Region. Except for Pr3 and C54, all previous assignments of methyl carbons were incorrect. From our results, we find the largest effect of protonation on the C47 signal, which shifts downfield by 1.3 ppm. The signals for both C20 and C54 shift downfield by 1.2 ppm. These ^{13}C signals could be affected both by the movement of nearby side chains and by the change in the proximity of the DMBz (see below).

Contrary to previous findings, B10 does not shift appreciably, and thus there is no evidence for "steric compression".[7] Our results also do not support the view that the ^{13}C shifts indicate greater flexibility for the eastern half of the corrin ring.[8] For example, the signal for C37 shifts relatively little on protonation, and the changes in chemical shift for C41 and C42 are comparable to those of C55. Rather, the changes in chemical shift we observed are greatest for the carbons on the C ring side chains, intermediate for those on the D and B rings, and smallest for those on the A ring. The largest effects are on the signals for carbons in side chains pointing toward the lower half of the molecule, as expected.

Effects of Changing Upper Axial Ligands

More recently, Brown and co-workers have evaluated structural changes in cobalamins based partly on the published tentative assignments.[24] This study focused on the nucleotide loop, and we will restrict our discussion to this region of the molecule. However, as will become evident, some of the signals assigned previously to the nucleotide loop were, in fact, from carbon atoms elsewhere in the molecule. Some aspects of the following discussion must be considered tentative since at this juncture, without a complete analysis of ^{13}C shifts for each alkylcobalamin, there may be errors in extrapolation of the coenzyme B_{12} assignments to those of other cobalamins. However, considerable clarification of problems denoted by Brown[24] emerges from our studies and merits description here.

It is known that ^{13}C shifts of axial ligands in organocobalt compounds can be influenced by through-bond electronic effects caused by electron donation to the electrophilic Co center and by through-space effects caused by Co and equatorial ligand anisotropy.[25] Brown introduced the idea that the electronic effect could be tentatively estimated as being a fraction of the effect of that of the powerful electrophile, H^+.[24] This latter effect was evaluated on the basis of changes in the DMBz chemical shift upon protonation of the DMBz nucleoside and nucleotide, α-ribazole and α-ribazole-3′-phosphate. Thus, according to this analysis, the Co centers in alkylcobalamins and vitamin B_{12} (cyanocobalamin) are ca. 10% and 45% as electrophilic as a proton, respectively. This order is reasonable.

Brown's results[24] for ^{13}C shifts on protonation of either the free ribazole or its nucleotide were similar except for R3. Corresponding shifts of the base-off form of B_{12} agree within 1 ppm with those for the free protonated nucleotide, except for B8 and B9 where the shifts for B_{12} are 1.0 and 1.3 ppm further downfield, respectively. Thus, the shifts for the protonated nucleotide appear similar regardless of whether it is covalently linked to the coenzyme or free in solution.

There are substantial chemical shift differences between the nucleotide loop in *base-on* B_{12} and the free unprotonated nucleotide, as might be expected. However, the shifts for only B2, B9, R1, R2, and R4 differ by ca. 1 ppm or more, with the biggest differences found for B9 and R2, which are upfield in the coenzyme by ca. 2 ppm. Significant trends with changes in the upper, axial ligand were found previously for cobalamins except for "R2" and R5. However, since R2 and Pr2 assignments were incorrectly interchanged, it is actually Pr2 and R5 which do not show significant trends with changes in the alkyl group. Previously, it was found that only "B6" of the nucleotide loop signals falls outside of the range expected between unprotonated and protonated ribazole phosphate. This discrepancy should now be attributed to B5, and only B5 of the DMBz ^{13}C signals appears to be significantly shifted in the opposite direction expected from protonation. This difference, plus an erratic pattern of shifts relative to that expected from the electrophilic effect, led Brown to postulate that Co anisotropy was responsible for the differences. We note, however, that the geometric term for Co anisotropy is quite similar for both B5 and B6.[24] Finally, since both B10 and B11 were incorrectly assigned, Brown's inability to account for the shift trends of "B10" and "B11" is explained.

On the basis of the R2 and R4 shifts, Brown suggested a considerable conformational change in the nucleotide ribose conformation on coordination of the DMBz for all of the cobalamins examined.[24] The R2 signal used was actually Pr2. However, even with the correct assignment, R2 is still considerably shifted (but now *up*field) compared to the shift for free ribazole-3′-phosphate. This result can be viewed as supporting the suggestion[24] of a conformational difference between ribazole-3′-phosphate and the nucleotide loop in base-on cobalamins. However, for R2, the difference in chemical shift between free and bound species becomes greater as the Co becomes more electrophilic, as in aquocobalamin, whereas for R4, the difference decreases. Thus, the changes in shift may reflect competing effects. Since the shifts for the nucleotide loop carbons in all of the protonated cobalamins are similar, the ribose ring likely has the same conformation in these species and in protonated ribazole-3′-phosphate.

^1H Chemical Shifts

^1H shift changes are most easily observed by comparison of the ^1H–^{13}C ^1J HMQC correlation spectra (see Figure 3 of this work and Figure 5 of ref 11). For base-on B_{12}, all of the methylene protons of the acetamide and propionamide side chains have chemical shifts between 1.7 and 2.7 ppm, with the exception of C41 and C42. One of the C41 and one of the C42 geminal proton signals occur upfield by ca. 1 ppm. From inspection of models, it is apparent that the C41–C42 side chain lies over the aromatic

(23) Glusker, P. J. In B_{12}; Dolphin, D., Ed.; Wiley: New York, 1982; Vol. 1, p 23.

(24) Brown, K. L.; Hakimi, J. M. *J. Am. Chem. Soc.* **1986**, *108*, 496.

(25) Stewart, R. C.; Marzilli, L. G. *Inorg. Chem.* **1977**, *16*, 424.

region of the DMBz; thus the unusual upfield shift for these protons is attributed to ring current effects of the DMBz. In contrast, no unusual upfield shifts are observed for the C41 or C42 protons of the base-off form, indicating that the DMBz has been displaced. It is also interesting to note that the chemical shift difference between the C49 geminal protons increased from ca. 0 ppm (overlap) in the base-on form to 0.35 ppm in the base-off form. For the remaining propionamides, the geminal proton signals for the terminal methylene (C31 and C42) overlap in the base-off form. Thus, it appears that the C48–C49 side chain undergoes reorientation on DMBz dissociation, consistent with the ^{13}C results.

Resonances of the corrin ring protons C3H, C8H, C13H, C18H, and C19H shift to a lower field by 0.13, 0.44, 0.54, 0.20, and 0.46 ppm, respectively, on DMBz dissociation. These downfield shifts probably reflect losses in electron density on removal of the electron-donating DMBz.

NOE and *J*-Couplings

Integrated intensities of NOE cross peaks and measurement of homonuclear *J*-couplings can provide valuable structural information as evidenced by numerous recent applications to polynucleotides and polypeptides.[26-30] Quantitative distance information can be obtained through analysis of transient NOE buildup data, and less precise distances can be derived from analysis of a single set of NOE data obtained by using a short mixing time. The first approach requires large amounts of spectrometer time and memory space and also relies on evolving computational methods currently not generally available. The main drawback of the second approach is the low intensity of cross peaks for the short mixing time and the fact that the extent of spin diffusion is unknown. However, this latter approach is more suited to our present capabilities, and our analysis proceeds along these lines. Thus, under the conditions employed the absence of an NOE signal may be due to (i) a large (> ca. 4 Å) interproton distance or (ii) short $T_{1\rho}$ values; however, the presence of an NOE cross peak provides unambiguous evidence for a short (< ca. 4 Å) interproton distance. At the contour levels drawn in Figure 2, cross peak intensities of ca. 1% of the diagonal peak area can be seen, and these cross peaks are summarized in the supplementary material. Cross peak intensities as low as ca. 0.3% were obtained from a detailed analysis of sections of the 2D data set, and selected signal intensities are summarized in Table III.

For the HMBC experiment, a decrease in proton T_2 leads to weaker correlation peaks, and comparisons of intensities between different samples must be made with caution. However, the ratios of correlation peak intensities for a given proton signal will be the same as long as the long-range ^1H–^{13}C coupling constants are unchanged.

Despite the above limitations, structural information can be obtained through careful analyses of signal intensities from the correlation experiments. Results for the different experiments are presented separately below.

^1H–^{13}C Multiple-Bond Coupling. The HMBC connectivity patterns and relative signal intensities were virtually identical for nearly all of the protons of base-on and base-off B_{12}. In particular, correlations between C3H, C8H, C13H, and carbons of the corrin ring were similar for the base-on and base-off forms. This similarity implies that no significant conformational changes have occurred at the A, B, and C rings of the corrin. This implication is consistent with the conclusions based on chemical shifts. For the D ring, no HMBC signals are observed for C19H of either the base-on or the base-off forms. C18H gives weak HMBC signals to C17 but not to C1, C19, or C16 in base-off B_{12}. Similarly, C18H does not give a correlation peak to C16 in base-on B_{12} but does give a very weak correlation peak to C1. (Correlation peaks with C19 and C17 could not be assigned exclusively to C18H in base-on B_{12} due to overlap between C18H and C60H_2.) Thus, these data provide little structural information for the D ring of the corrin.

Some differences are observed for the ribose protons and for the *e*-propionamide side chain. Thus, C13H gives a relatively intense correlation peak to C49 in base-on B_{12} whereas no such

Table III. Selected Interproton Distances (Å) and 2D NOE Cross Peak Intensities for the Base-On and Base-Off Forms of Coenzyme B_{12}[a]

spin pair	distance[b]	intensity	
		base-on	base-off
A8–A11	3.91	1.9	1.9
A8–A12	2.85	1.9	1.5
A8–A13	2.24	1.7	1.9
A8–A14	4.57		
A8–A15′	4.44		
A8–A15″	3.34	0.20	0.26
A8–C46	3.36	0.27	0.25
A11–C54	2.92	1.1	0.64
A11–C53	3.56		
A11–C46	3.75	1.3	2.1
A14–C19	2.02	1.2	1.7
A14–C54	1.99	*d*	0.42
A14–C26′	2.93		
A14–C26″	3.77		
A14–C60′	3.96		
A14–C46	4.50	1.3	1.0
A15″–A15′	1.71	10.0	10.0
A15″–C37″	2.52	0.31	0.25
A15″–C37′	3.54	0.30	0.11
A15″–C26′	5.92		
A15″–C26″	4.40	0.18	0.16
A15″–C46	3.32		
A15″–C10	3.85		
A15′–C26′	2.82	*c*	0.19
A15′–C26″	4.49		
A15′–C37″	3.05		
A15′–C37′	3.21		
A15′–C19	3.20	2.9	3.2
A15′–C35	3.85		
A15′–C3	4.12		
C54–C19	2.39	2.8	3.1
B4–C20	3.19	0.61	
B4–C35	3.77	0.69	
B4–C36	3.37	0.31	
B4–C30′	2.82	1.5	
B4–C30″	3.11	0.59	
B4–C31′	4.90		
B4–C31″	5.50		
B4–C41′	4.09		
B4–C41″	2.42	2.8	
B4–C18	6.13		
B2–R1	3.87	0.39	0.44
B2–R2	4.42		
B2–R3	4.83		
B2–R4	2.69	1.4	0.79
B2–C20	3.00	0.59	
B2–C48′	2.41	2.9	
B2–C48″	2.64	2.9	
B2–C49′	4.63		
B2–C49″	5.05		
B2–C18	4.07		
B7–R1	2.31	2.9	2.2
B7–R2	3.20	0.20	0.18
B7–B11	2.35	1.9	1.9
B10–C35	2.65	0.19	
C20–B7			0.37
C20–R1			0.19
C20–B11			0.39

[a] Integrated cross peak areas relative to A15′–A15″ (1.71 Å) = 10.0. [b] From neutron diffraction data (ref 38). For methyl groups, only the distance for the "nearest" protons is given. [c] Obscured by the intense A15′–A14 cross peak. [d] Obscured by nearby cross peaks.

(26) Williamson, M. D.; Havel, T. F.; Wuthrich, K. *J. Mol. Biol.* **1985**, *182*, 281.
(27) Feigon, J.; Leupin, W.; Denny, W. A.; Kearns, D. R. *Biochemistry* **1983**, *22*, 5930.
(28) Wemmer, D. E.; Chou, S.-H.; Hare, D. R.; Reid, B. R. *Biochemistry* **1984**, *23*, 2262.
(29) Broido, M. S.; James, T. L.; Zon, G.; Keepers, J. W. *Eur. J. Biochem.* **1985**, *150*, 117.
(30) Bruch, M. D.; Noggle, J. H.; Gierasch, L. M. *J. Am. Chem. Soc.* **1985**, *107*, 1400.

signal is observed in the base-off form. This implies a change in the C13H–C13–C48–C49 torsion angle, consistent with the chemical shift results. R2H and R3H display HMBC correlation peaks in the base-on data whereas no similar connectivities are observed in the base-off data. This difference implies that some structural changes occur in the DMBz-attached ribose on dissociation of the DMBz and is supported by the associated changes in chemical shifts and coupling constants.

^{1}H–^{1}H Coupling. The only coupled protons on the corrin ring which could provide information on changes in ring pucker are C18H and C19H. For base-off B_{12}, a value of 10.2 Hz was measured for this coupling (Table II). For the base-on form, the C18H signal overlapped with $C60H_2$ signals, the C19H signal was unusually broad (ca. 6-Hz line width) and overlapped with R2H, and the coupling could not be measured from the 2D-J spectrum. A coupling constant of 10.5 Hz was measured using a *z*-filtered variation of the 1D HOHAHA experiment.[31,32] Coupling constants for the adenosyl ribose are typical for a sugar which is predominantly in the N conformation[33] as observed in the solid. In addition, the large coupling for A15H″–A14H (8.9–9.2 Hz) and the small (unresolved) coupling for A15H′–A14H are consistent with the respective torsion angles (−169° and 75°) observed in the solid.

Coupling constants for the adenosyl ribose remain virtually unchanged on dissociation of the DMBz (Table II). On the other hand, large changes are observed for some of the ^{1}H–^{1}H coupling constants of the DMBz-attached ribose and for the propanolamine side chain. ^{1}H–^{1}H couplings are differentiated from ^{1}H–^{31}P couplings in the 2D-J spectrum (Figure 6), where homonuclear couplings (but not heteronuclear couplings) are resolved in the *F*1 dimension. Most significantly, $^3J_{R1H-R2H}$ and $^3J_{R3H-R4H}$ change from 3.0 and 8.9 to 5.2 and 3.1 Hz, respectively, on DMBz dissociation. This suggests that the DMBz-attached ribose changes from a predominantly N to a predominantly S geometry.[33] On DMBz dissociation, values for $^3J_{Pr1H'-Pr2H}$ and $^3J_{Pr1H''-Pr2H}$ change from <0.9 and 14.4 to 5.2 and 3.9 Hz, respectively. This indicates that the average Pr1H′–Pr1–Pr2–Pr2H and Pr1H″–Pr1–Pr2–Pr2H torsion angles have changed from −64° and 175° (observed in the solid) to new angles which are relatively similar to each other.[34-37]

^{1}H–^{31}P Coupling. Pr2H–P couplings are nearly identical for base-on (7.1 Hz) and base-off (7.0 Hz) B_{12}. Couplings to Pr1H′ and $Pr3H_3$, evidenced in the ^{1}H–^{31}P spin-echo difference spectrum of base-on B_{12}[12], could not be resolved. A small change (0.7 Hz) is observed in the R3H–P coupling constant (Table II). These results imply that the R3H–R3–O–P torsion angle changes on DMBz dissociation whereas the Pr2H–Pr2–O–P torsion angle either does not change significantly or changes to a different angle which gives the same coupling constant.

^{13}C–^{31}P Coupling. For the propanolamine, no couplings are observed for Pr1–P whereas values for $^2J_{Pr2-P}$ and $^3J_{Pr3-P}$ change from 6.2 and 4.4 to 5.5 and 3.3 Hz, respectively, on DMBz dissociation (Table II). These changes are relatively small. In contrast, values for $^3J_{R2-P}$, $^2J_{R3-P}$, and $^3J_{R4-P}$ change from <0.9, 3.7, and 9.1 to 3.3, 4.4, and 2.6 Hz, respectively. These changes in coupling reflect, at least in part, changes in sugar pucker.

In summary, the coupling constant data indicate that structural changes on DMBz dissociation occur primarily at the *e* side chain, the DMBz-ribose, and the propanolamine side chain. No evidence is found for a change in the corrin ring pucker.

^{1}H–^{1}H NOE. Structurally relevant NOE cross peak areas and associated interproton distances derived from neutron diffraction studies[38] are listed in Table III. Included are relatively weak (areas to ca. 0.3% of the diagonal) NOE signals obtained from slices of the 2D NOE data. In our analysis of the NOE results, no attempts area made to quantitate distances or derive a solution structure. In fact, as will be shown, much of the NOE data indicate that the structures are not rigid in solution and that conformational changes occur which are sometimes in fast exchange on the NMR time scale. Instead, the NOE data are analyzed for compatibility with the coupling constant (above) and distance data.

Base-On B_{12}

A number of cross peaks for protons of the adenosyl and the corrin are observed that provide information on the relative orientation of these groups, Table III. The following NOE cross peaks are of particular interest: A8H–$C46H_3$; A11H–$C54H_3$ and –$C46H_3$; A14H–C19H and –$C46H_3$; A15H″–C37H″, –C37H′, and –C26H″; and A15H′–C19H. These signals represent cross-relaxation between five protons of the adenosyl and all four "sides" of the corrin ring. The presence of these signals provides strong evidence that the orientation of the adenosyl with respect to the corrin is roughly the same in solution as it is in the solid state. Relatively small structural differences and dynamic effects are reflected in the relative NOE intensities (Table III) and by the presence and/or absence of expected signals based on the solid-state data. For example, interproton distances of ca. 3–4 Å were obtained in the solid for A11H–$C53H_3$; A14H–$C26H_2$ and –$C60H_2$; A15H″–$C46H_3$ and –C10H; and A15H′–$C37H_2$, –$C35H_3$, –C3H, and –$C60H_2$. These pairs do not exhibit NOE cross-relaxation. Of more significance are the cross peak intensities for A14H–$C46H_3$, A14H–C19H, and A15H′–C19H of 1.3, 1.2 and 2.9, respectively. Comparison with the respective distances of 4.50, 2.02, and 3.20 Å suggests a difference in the average orientation of the adenosyl relative to the corrin for the solid-state and solution species. Since the A14H–A15H′ and A14H–A15H″ couplings are consistent with the associated torsion angles observed in the solid, the structural changes probably result from rotation about the Co–C bond. Inspection of models indicates that a single, static conformation alone cannot account for the NOE intensities observed. A two-state model which qualitatively fits our data better is one where the adenosyl exists part of the time in a conformation similar to that found in the crystal structure and part of the time with the adenosyl rotated counterclockwise ca. 50° about the Co–C bond (when viewed from the adenosyl).

Base-Off B_{12}

Interestingly, the NOE intensities for cross peaks between the adenosyl and the corrin are remarkably similar for the base-on and base-off forms (Table III). First consider the adenosyl. NOE cross peaks between A8H and protons of the adenosyl ribose are virtually identical with those of the base-on form, as is the A8H–$C46H_3$ cross peak. Cross peaks between protons of the adenosyl ribose and most of the protons of the corrin and its side chains are also similar to those observed for base-on B_{12}; e.g., peak intensities of 2.9 and 3.2 for A15H′–C19H, 1.3 and 1.0 for A14H–$C46H_3$, 1.2 and 1.7 for A14H–C19H, and 0.31 and 0.25 for A15H″–C37H″ are observed for base-on and base-off B_{12}, respectively. *Thus, it is clear that the solution conformation of the adenosyl and the orientation of the adenosyl with respect to the corrin ring are the same in both the base-on and base-off species.* In addition, the cross peak between C19H and $C54H_3$ remains virtually unchanged on DMBz dissociation (2.8–3.1), which implies that the conformation of the corrin D ring does not change. This is consistent with the relatively unchanged C19H–C18H coupling constant (10.5–10.2 Hz).

Cross peaks between protons of the DMBz and its attached ribose indicate that the DMBz is in an anti configuration relative to the ribose, similar to that observed in base-on B_{12}. As expected,

(31) Davis, D. G.; Bax, A. *J. Am. Chem. Soc.* **1985**, *107*, 7197.
(32) Subramanian, S.; Bax, A. *J. Magn. Reson.*, in press.
(33) Altona, C. *Recl. Trav. Chim. Pays-Bas* **1982**, *101*, 413. Note: In B_{12}, the DMBz-ribose contains an α-glycosyl C–N linkage whereas DNA contains a β-linkage. This difference explains the small discrepancy between the observed and theoretical R1H–R2H couplings.
(34) Karplus M. *J. Chem. Phys.* **1959**, *30*, 11.
(35) Karplus M. *J. Am. Chem. Soc.* **1963**, *85*, 2870.
(36) Bothner-By, A. A. *Adv. Magn. Reson.* **1965**, *1*, 195.
(37) Becker, E. D. *High Resolution NMR*, 2nd ed.; Academic: New York, 1980; p 102.
(38) Finney, J. L.; Lindley, P. F.; Savage, H. F. J. submitted for publication in *Acta Crystallogr., Sect. A: Found. Crystallogr.*

none of the cross peaks observed between the DMBz and corrin protons in base-on B_{12} are observed in the base-off species. However, new cross peaks are observed that provide key information on the location of the DMBz in base-off B_{12}. Thus, cross-relaxation is observed between $C20H_3$ and B7H, R1H, and $B11H_3$, Table III. No cross peaks are observed between protons of the corrin and B4H or $B10H_3$. These results indicate that the DMBz is repositioned upside down in base-off B_{12} with B7H, R1H, and $B11H_3$ in the proximity of $C20H_3$. Of course, we expect there to be a considerable amount of motional freedom for the DMBz, and we do not intend to propose a particular static structure. In addition to these new cross peaks, R1H gives a cross peak with Pr2H and R2H gives a cross peak with $Pr3H_3$, confirming the structural changes in the propanolamine–phosphate–ribose moiety indicated above.

Summary

Following our reassignment of many ^{13}C signals of base-on and base-off B_{12}, we were able to reinterpret shift changes which accompany DMBz dissociation and changes in alkyl donor ability. A single, static structure cannot account for all of the NOE intensities observed between protons of the adenosyl and the corrin. A dynamic equilibrium between at least two conformations is needed to account for all of the NOE data; one conformation is similar to that of the crystal structure, and in the other conformation, the adenosyl is rotated ca. 50° counterclockwise about Co–C bond (when viewed from the adenosyl). The NOE and scalar coupling data indicate that this solution structure is remarkably similar in the base-on and base-off species, and no evidence was found to indicate a change in corrin ring pucker on DMBz dissociation. The NOE data indicate that the DMBz is repositioned upside down in the base-off form with B7H, R1H, and $B11H_3$ in the proximity of $C20H_3$.

The lack of a conformational change for the corrin ring on DMBz dissociation seemed surprising to us at first since alkylcobalamins containing bulky alkyl groups (such as isopropyl or neopentyl) are known to be more stable in the base-off form. This increase in stability has been attributed to decreased steric interactions between the alkyl and the corrin. Here, our data indicate that the corrin is not as flexible as might be expected based on studies of B_{12} model compounds and that steric interactions between the alkyl and the corrin are probably relatively unchanged on DMBz dissociation (due to the lack of an observed change in corrin–adenosyl NOE intensities). Instead, the increased stability of the base-off species may be due to the inability of the protonated DMBz to stabilize Co(II) subsequent to homolysis. Further homolysis studies on base-on and base-off alkylcobalamins are clearly in order.

Although structural data for five-coordinate Co(III) complexes are rare,[10] such results demonstrate that the Co is displaced toward the attached carbon and out of the plane defined by the four donor atoms of the equatorial ligand, resulting in a lengthening of the distances between the coordinated alkyl group and the equatorial ligand. Since such effects are not observed for B_{12}, our results support the concusion[8] that a water molecule assumes the sixth coordination site in base-off B_{12}.

Clearly, this work demonstrates both the powerful utility of modern NMR methods and the need for additional work. In future studies, we hope to obtain quantitative information on the Co–N(DMBz) distance and the orientation of the DMBz with respect to the corrin ring for alkylcobalamins and, if possible, for a holoenzyme.[39]

Experimental Section

Coenzyme B_{12} (16 mg, Sigma) was stirred into D_2O (0.35 mL, 99.8%, Merck) containing 10 mM phosphate buffer. The pH* was then adjusted to 1.9 by addition of DCl, and the sample was lyophilized. The sample was then dissolved in 99.96% D_2O (0.35 mL, Merck). After NMR measurements, the pH* was measured to be 2.1. All of the 2D NMR experiments were performed using a modified Nicolet NT-500 spectrometer, equipped with a Cryomagnet Systems ^1H probe with a broadband (^{15}N–^{31}P) decoupling coil for irradiation of ^{13}C. The temperature was 20 °C, and all experiments were carried out without sample spinning. Proton and carbon chemical shifts were referenced to internal trimethylsilyl 3-propionate (TSP); the exact carbon shifts were measured from the 1D spectrum, obtained on a JEOL GX400 spectrometer (100.5 MHz, ^{13}C) using a 50-mg sample in a 10-mm sample tube (2.5-mL sample volume).

Details on the optimization of the 2D experiments have been published previously.[11] The parameters used in this work are as follows. *HMQC*: 2 × 300 × 1024 data matrix size (two separate sets of data, with 300 data points in t_1 and 1024 data points in t_2); 32 scans (preceded by 2 dummy scans) per t_1 value; pulse delay = 0.9 s; 12 W of ^{13}C rf power; 6- and 20-Hz Gaussian filtering in t_2 and t_1, respectively. *HMBC*: 300 × 2048 data matrix size; 128 scans (preceded by 2 dummy scans) per t_1 value; pulse delay = 1.5 s; 15 W of ^{13}C rf power; 70-μs (82°) ^{13}C pulse width; Δ_1 and Δ_2 durations of 3.4 and 55 ms, respectively; sine bell filter and 20-Hz Gaussian filtering in t_2 and t_1, respectively. *HOHAHA*: 2 × 350 × 1024 data matrix size; 8 scans per t_1 value; pulse delay = 1.8 s; MLEV-17 mixing time = 52 ms, preceded and followed by 2.5-ms trim pulses; 6-W rf power corresponding to 35-μs 90° ^1H pulse width; 6- and 9-Hz Gaussian filtering in t_2 and t_1, respectively. *Spin-Locked NOE*: 2 × 350 × 1024 data matrix size; 64 scans per t_1 value; pulse delay = 1.8 s; 5-kHz rf field strength (50-μs 90° pulse width); mixing time = 200 ms; 6- and 9-Hz gaussian filtering in t_2 and t_1, respectively. *J-Resolved*: 64 × 4096 data matrix size with zero-filling to 128 points in t_1 and 8192 points in t_2; 1.28-s acquisition time in t_2; 16 scans per t_1 value; pulse delay = 2 s; 5-Hz exponential line narrowing plus 4-Hz Gaussian line broadening in t_1 and t_2.

Acknowledgment. We are grateful to Dr. Hugh Savage (National Bureau of Standards) for providing the unpublished neutron diffraction data and to Rolf Tschudin (N.I.H) for continuous technical support. L.G.M. thanks the NIH for financial support, Grant GM 29225. We also appreciate the help of Rick Venable (F.D.A.) for assistance in using Dr. Richard Feldman's molecular graphics system (N.I.H.).

Supplementary Material Available: Table SI containing HOHAHA, NOE, and HMBC connectivities used for ^1H and ^{13}C spectral assignments; Figures S1–S10 of COSY and HOHAHA spectra showing the ^1H–^1H *J*-networks of base-off B_{12}, downfield ^{13}C HMQC and HMBC spectra of base-off B_{12}, and part of the ^1H–^1H 2D-J spectrum of base-on B_{12} (15 pages). Ordering information is given on any current masthead page.

(39) After this paper was submitted, evidence was presented [Brown, K. L. Presented at the Northwest Regional Meeting of the American Chemical Society, Portland, OR, June 1986] for hydrogen bonding between the *e* side chain and the unprotonated DMBz.